Large-amplitude jumps and non-Gaussian dynamics in highly concentrated hard sphere fluids

Erica J. Saltzman* and Kenneth S. Schweizer†

Department of Materials Science and Seitz Materials Research Laboratory, University of Illinois, 1304 West Green Street, Urbana, Illinois 61801, USA

(Received 5 March 2008; published 23 May 2008)

Our microscopic stochastic nonlinear Langevin equation theory of activated dynamics has been employed to study the real-space van Hove function of dense hard sphere fluids and suspensions. At very short times, the van Hove function is a narrow Gaussian. At sufficiently high volume fractions, such that the entropic barrier to relaxation is greater than the thermal energy, its functional form evolves with time to include a rapidly decaying component at small displacements and a long-range exponential tail. The "jump" or decay length scale associated with the tail increases with time (or particle root-mean-square displacement) at fixed volume fraction, and with volume fraction at the mean α relaxation time. The jump length at the α relaxation time is predicted to be proportional to a measure of the decoupling of self-diffusion and structural relaxation. At long times corresponding to mean displacements of order a particle diameter, the volume fraction dependence of the decay length disappears. A good superposition of the exponential tail feature based on the jump length as a scaling variable is predicted at high volume fractions. Overall, the theoretical results are in good accord with recent simulations and experiments. The basic aspects of the theory are also compared with a classic jump model and a dynamically facilitated continuous time random-walk model. Decoupling of the time scales of different parts of the relaxation process predicted by the theory is qualitatively similar to facilitated dynamics models based on the concept of persistence and exchange times if the elementary event is assumed to be associated with transport on a length scale significantly smaller than the particle size.

DOI: 10.1103/PhysRevE.77.051504 PACS number(s): 61.20.Lc, 61.20.Ja, 05.40.Ca, 82.70.Kj

I. INTRODUCTION

The heterogeneous and non-Gaussian *single-particle* dynamics of glassy colloidal suspensions [1–11] and supercooled liquids [12–24] has recently been the subject of intense experimental, theoretical, and simulation interest. A host of dynamical fluctuation phenomena at the single-particle level exist, which emerge even in the putative dynamical "precursor" regime probed in colloid experiments and computer simulations where ideal mode-coupling theory (MCT) [25,26] provides a good description of many ensemble-average "mean" dynamical properties [1]. However, ideal MCT severely underpredicts dynamical fluctuation effects such as the decoupling of diffusion and relaxation, large non-Gaussian parameters, and the non-Fickian wave-vector dependence of the incoherent dynamic structure factor relaxation times, and does not predict at all the emergence of exponential tails in the real-space single-particle van Hove function [1,18]. All these phenomena likely arise from a crossover in transport mechanism to an intermittent activated hopping dynamics [1,8].

The focus of the present paper is the van Hove function [27], $G_s(r,t)$, which quantifies the distribution of single-particle displacements, r, over the time interval t. An exponential tail feature in $G_s(r,t)$ has been observed in recent computer simulations and experiments [1,4–24]. The key, nearly universal, physics involves highly non-Gaussian jumplike motions on a *microscopic* length scale, which leads to a bifurcation of mobility into fast and slow subpopulations [14]. We note that jump motions in dense liquids have been discussed in various contexts for over half a century [28–30]. Some recent analyses of the problem are based on kinetically constrained models (KCMs) [14,15,23,24], which emphasize dynamic heterogeneity and facilitation. The KCMs are conceptually akin to specific forms of the continuous random-walk model (CTRW) [31], and involve multiple parameters determined by fitting experimental or simulation data. In this exercise, the definition of a discrete particle "hop" must be postulated [14,15,32,33].

Here we study the real-space van Hove function of dense hard sphere fluids based on our microscopic stochastic nonlinear Langevin (NLE) theory of activated dynamics [34,35]. Extensive quantitative confrontation of this approach with computer simulation and colloid experiments for both average properties [8,34,36] and non-Gaussian dynamical fluctuation phenomena [1,8,37] has provided evidence of its physical soundness. In Sec. II, the basics of the theory are summarized. Predictions for the van Hove function over a wide range of volume fractions and time scales are presented in Sec. III. The relationship of our approach to classic [30] and recent [14,15,24] models for particle hopping is the topic of Sec. IV. Section V discusses the issue of decoupling of the time scales of different parts of the relaxation process, and the possible relationship of our approach to the persistence and exchange time concepts of KCM models [23,24,38]. The paper concludes with a brief discussion in Sec. IV.

II. THEORETICAL BACKGROUND

Our theory has been heuristically motivated on physical grounds [34], and derived from time-dependent statistical

*Present address: Department of Polymer Science and Engineering, University of Massachusetts, Amherst, MA.

†Author to whom correspondence should be addressed; kschweiz@uiuc.edu

mechanics [35]. It is built on a locally solid-state, or inhomogeneous fluid, picture of slow dynamics. The interparticle force contribution to the single-particle stochastic nonlinear Langevin equation is rendered tractable based on a dynamic density-functional theory local equilibrium idea [39]. This allows the instantaneous caging forces to be renormalized in an effective potential manner based on knowledge of the structure factor, $S(k)$. Dynamic closure is achieved by adopting an approximate relation between one- and two-particle dynamics. The resultant nonlinear Langevin equation of motion for the instantaneous scalar particle *displacement* from its initial position, $r(t)$, is given in the overdamped limit by [34,35]

$$\zeta_s \frac{\partial r(t)}{\partial t} = -\frac{\partial F_{\rm eff}[r(t)]}{\partial r(t)} + \delta f(t), \tag{1}$$

where the random force satisfies $\langle \delta f(0)\delta f(t)\rangle = 2k_BT\zeta_s\delta(t)$, and $\zeta_s = k_BT/D_s$ is the short time friction constant. For hard sphere colloids [40], $\zeta_s = \zeta_0 g(\sigma)$ is the dilute Stokes-Einstein friction constant, σ is the hard sphere diameter, and an essentially exact expression [34] for the contact value of the radial distribution function, $g(\sigma)$, is employed. The effective or nonequilibrium free energy is

$$\beta F_{\rm eff}(r) = -3\ln(r) - \int \frac{d\vec{k}}{(2\pi)^3}\rho C^2(k)S(k)[1+S(k)]^{-1} \times \exp\left[-\frac{k^2r^2}{6}[1+S^{-1}(k)]\right] \equiv \beta F_{\rm ideal} + \beta F_{\rm excess}, \tag{2}$$

where $\beta = 1/(k_BT)$ is the inverse thermal energy, $C(k) = [1-S(k)]/\rho$ is the Fourier-transformed direct correlation function calculated using Percus-Yevick theory [41], and ρ is the number density. The nonequilibrium free energy is a monotonically decreasing function of particle displacement for $\phi \le 0.432$, which defines the "normal" fluid regime. A minimum in $F_{\rm eff}(r)$ at the "localization length," $r = r_L$, first emerges at $\phi_c = 0.432$ [34], which defines a simplified or "naive" [42] mode-coupling theory (NMCT) nonergodicity transition. In our approach, this ideal glass transition signals the onset of transient localization, emergence of an entropic barrier of height F_B, and a crossover to activated dynamics. Examples of $F_{\rm eff}(r)$ for the volume fractions presently studied are shown in Fig. 1. The barrier is $\sim k_BT$ at $\phi = 0.5$, and grows to $6.7k_BT$ at $\phi = 0.57$. In the spirit of transition state theory, the "hopping distance," defined as the difference between the location of the barrier and localization well, increases monotonically with volume fraction. Throughout the paper, all lengths are in units of the sphere diameter and all times are in units of $\tau_0 = \sigma^2/D_0$.

Equations (1) and (2) are based on a solid-state-like picture of a dense fluid and cannot be valid at arbitrarily long times or displacements. A dynamical crossover to an irreversible, linear, three-dimensional Langevin equation description is invoked by modifying Eq. (1) as [8,35]

$$-\frac{\partial F_{\rm eff}}{\partial r(t)} \to -\zeta_{\rm hop}(\phi)\frac{\partial \vec{r}}{\partial t}. \tag{3}$$

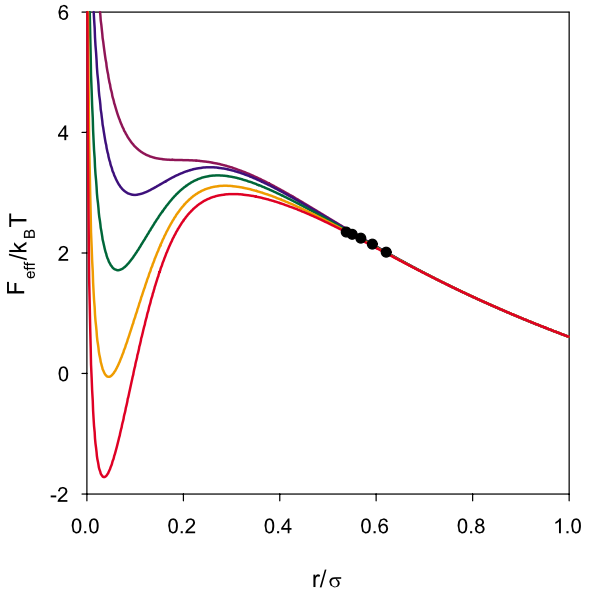

FIG. 1. (Color online) Effective free energy in units of the thermal energy as a function of particle displacement for volume fractions $\phi = 0.43$, 0.465, 0.5, 0.53, and 0.55 (from top). Circles mark the reaction point [8], which occurs at a displacement that decreases with volume fraction.

The hopping friction constant accounts for the *mean* frictional resistance associated with the barrier crossing or cage escape process. To quantitatively implement this idea, a "reaction point," $r^\dagger$, is *a priori* calculated to correspond to the displacement at which the localizing cage force becomes negligible. Various formulations of the reaction criterion all yield [8] $r^\dagger \simeq 0.5-0.6$, and are indicated in Fig. 1. The reaction point is substantially beyond the barrier at $r_B = 0.3-0.4$. The transition in dynamical description is executed on a single-trajectory basis, and trajectory propagation after the reaction event is described by an *ensemble-averaged* friction constant, $\zeta_s \to \zeta_s + \zeta_{\rm hop}$, where

$$\frac{1}{\zeta_{\rm hop}} = \frac{1}{N}\sum_{i=1}^{N}\frac{1}{\zeta_{{\rm hop},i}}. \tag{4}$$

The trajectory friction constant $\zeta_{{\rm hop},i}/k_BT = 6t_i^\dagger/r^{\dagger 2}$, where $t_i^\dagger$ is the time for the ith trajectory to pass the reaction point. Calculations are performed for $N = 40\,000$ trajectories. The "hopping diffusion constant" is $D_{\rm hop} = k_BT/\zeta_{\rm hop}$ and the long-time diffusion constant is $D = k_BT/(\zeta_s + \zeta_{\rm hop})$.

Numerical solutions of the NLE [8,37] have recently been obtained for $0.4 \le \phi \le 0.57$. The structural or α relaxation time, τ^*, is defined as $F_s(k^*, t=\tau^*) = e^{-1}$, where F_s is the incoherent dynamic structure factor and k^* is the cage peak wave vector of $S(k)$. Over the range $0.4 \le \phi \le 0.57$, the α time increases by three orders of magnitude. Many non-Gaussian dynamical fluctuation effects are predicted, including the following results most relevant to the present work. (i) Significant decoupling of the volume fraction dependence of the diffusion constant, D, and α time for $\phi > 0.5$. (ii) A spatial scale dependence of the decoupling of diffusion and relaxation characterized by a crossover length, ξ_D, that in-

creases linearly with ϕ and scales with the decoupling factor as $\xi_D \propto \sqrt{D\tau^*}$. (iii) The dimensionless distribution function, $P(r,t) \propto (r/\sigma)^3 G_s(r,t)$, broadens from Gaussian in the normal fluid regime to a bimodal form at intermediate times and high volume fractions. These and other non-Gaussian dynamical fluctuation predictions compare favorably with colloid experiments and simulations [1,8].

Our description of activated motion is based on a *spatially continuous* "dynamical landscape," not a discrete "hop." The barrier crossing and reaction events involve time scales that are distributed reflecting their thermal noise-driven nature [8]. The origin of decoupling is *not* a consequence of computing different moments of a common static distribution function. Moreover, "hopping events" are not irreversible since barrier recrossings, important under high friction conditions, are taken into account. However, a mean dynamical "constraint release" idea enters via the reaction point concept. This should be viewed as an approximate description of the inevitable crossover to Fickian diffusion at long times and distances. The idea that particle mobility grows with increasing time and spatial displacement, a cornerstone of coarse-grained facilitated or kinetically constrained models [23,24,28], is present at an elementary level.

III. NUMERICAL RESULTS

A. Van Hove function

The dimensionless displacement distribution function, $P(r,t) \equiv 4\pi \ln(10) r^3 G_s(r,t)$, is shown in two different plotting formats in Fig. 2. The vertical axis is left as an arbitrary scale since the numerical magnitude of $P(r,t)$ is slightly affected by the histogram bin size; moreover, an absolute scale is not necessary for any of the issues we will address. Note that if the dynamics were perfectly Gaussian, then the shape and peak height of $P(r,t)$ would be time-independent, while the peak location would increase diffusively with time. For ϕ=0.55 [Fig. 2(a)], $P(r,t)$ evolves from a single small-displacement peak at short times to a bimodal form at intermediate times and a single large-displacement Gaussian distribution at long times. The bimodality indicates mobility bifurcation and is maximized for times of order the α relaxation time, a trend most apparent in the logarithmic representation. Figure 2(b) shows the displacement distributions for several ϕ at the α time. The bimodality becomes more pronounced with increasing volume fraction. The qualitative features of our displacement distributions agree with simulations [8]. This representation of the van Hove function as $P(r,t)$ more clearly exposes the strong mobility bifurcation, although, of course, the exponential tail feature of $G_s(r,t)$ carries the same information.

To expose the exponential tail feature in the traditional manner, calculations of $G_s(r,t)$ are given in Fig. 3 in a log-linear representation. At very short times, the van Hove function is well described as a narrow Gaussian with no tail since all particles are caged. At longer times, the van Hove function retains its rapidly decaying form at small displacements but also develops a long-range exponential tail. The length scale associated with the tail increases monotonically with time [or root-mean-square particle displacement (MSD)] at

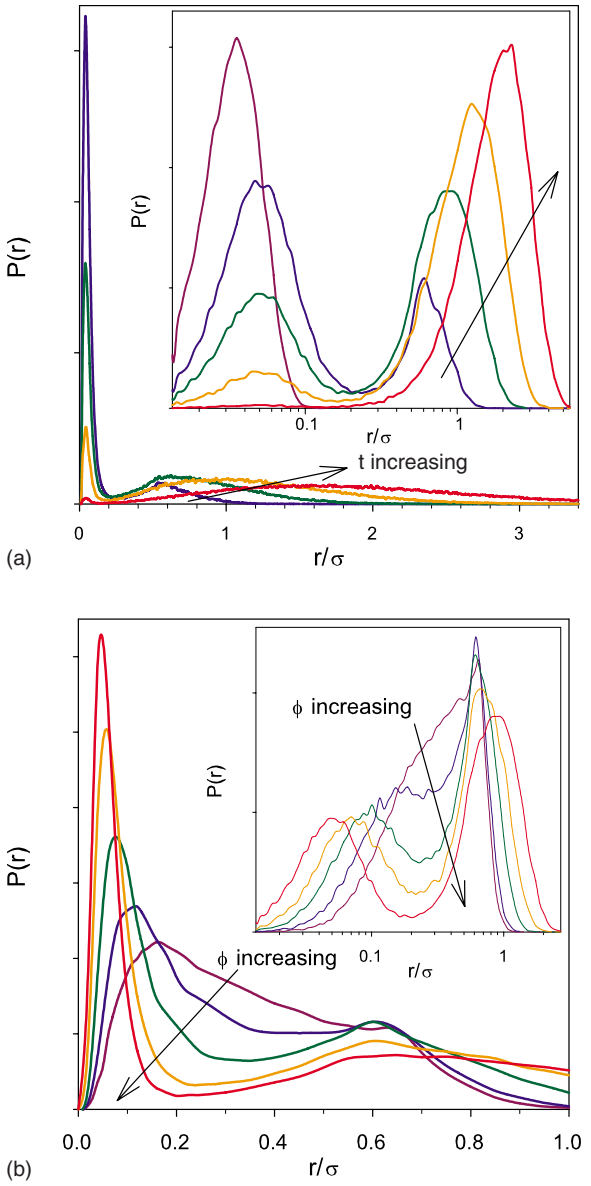

FIG. 2. (Color online) (a) Linear-linear plot of the displacement distribution (with linear bins, arbitrary vertical scale) for ϕ=0.55, at times corresponding to (from left) $\langle r^2 \rangle^{1/2} = r_B$, $t = \tau^*$, the analytic Kramers time [34] $t = \tau_K$, and $\langle r^2 \rangle^{1/2} = 2$. Inset: linear-log displacement distribution (with logarithmic bins) for the same system and conditions as in the main panel as well as $\langle r^2 \rangle^{1/2} = r_L$ (leftmost curve). The arrow points in the direction of increasing time. (b) Linear-linear plot of displacement distribution (with linear bins) at the α relaxation time for ϕ=0.43, 0.465, 0.5, 0.53, and 0.55. Inset: corresponding linear-log plots. The arrow points in the direction of increasing volume fraction.

fixed volume fraction [Fig. 3(a)], and with volume fraction at the ϕ-dependent α time [Fig. 3(b)]. We note that even at the longest times we have studied, $G_s(r,t)$ is not precisely Gaussian, as also found in experimental studies [33,34]. The linear fits in Fig. 3 demonstrate that the exponential decay, $G_s(r,t) \propto e^{-r/\lambda}$, works well at intermediate times, and also at "long" times as defined by a root MSD out to two particle diameters. For these longest times, the van Hove function at very large displacements [very small amplitudes of $G_s(r,t)$]

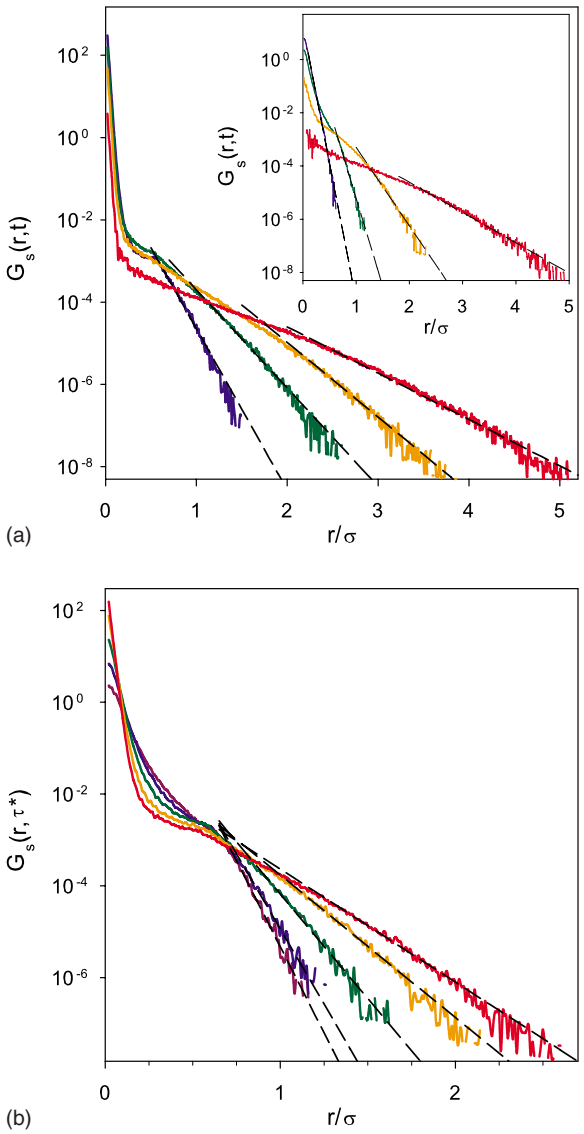

FIG. 3. (Color online) (a) Log-linear plot of the van Hove function for ϕ=0.55 at times corresponding to (from left) $\langle r^2\rangle^{1/2}=r_B$, $t=\tau^*$, the analytic Kramers time $t=\tau_K$, and $\langle r^2\rangle^{1/2}=2$. Dashed lines are exponential fits to the tails: $G_s(r,t)\sim e^{-r/\lambda}$. Inset: log-linear plot of the van Hove function for ϕ=0.43, at times corresponding to (from left) $\langle r^2\rangle^{1/2}=0.19$ [inflection point of $F_{\rm eff}(r)$], $t=\tau^*$, $t=\tau_K$, and $\langle r^2\rangle^{1/2}=2$. (b) Log-linear plot of van Hove distribution at the α relaxation time for volume fractions (left to right) ϕ=0.43, 0.465, 0.5, 0.53, and 0.55. Dashed lines are exponential fits to tails: $G_s(r,\tau^*)\sim e^{-r/\lambda^*}$.

exhibits a downward deviation from the exponential fit, which indicates the onset of a crossover to Fickian behavior. The characteristic length scale, λ, is a function of both elapsed time and volume fraction. It has traditionally been referred to as a "jump length" to emphasize that its physical origin is an activated hopping motion [28–30].

The basic features of the theoretical results in Fig. 3 are in qualitative accord with recent simulations [14] that find an exponential tail at intermediate times down to $G_s(r,t)\sim 10^{-8}-10^{-7}$, roughly the same range as our calculations. However, there are quantitative differences. The most apparent is that the exponential tail typically emerges in simulations when $G_s(r,t)\sim 0.001-0.01$, which is somewhat larger than for our results. A more significant difference is that the crossover from Gaussian to exponential form is smoother in simulation, and the shoulder and curve crossings in Fig. 3 are not evident. This likely reflects our oversimplified representation of the crossover from the NLE description to Fickian diffusion.

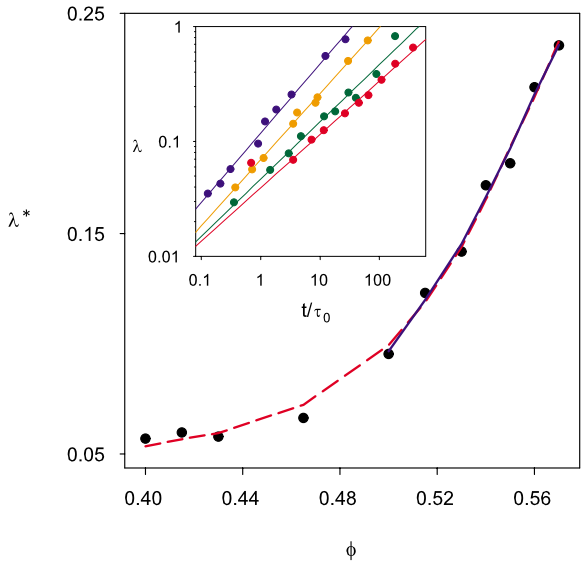

FIG. 4. (Color online) Exponential decay length for the van Hove distribution at the α relaxation time, τ^*, as a function of volume fraction (points). Linear fit to the diffusive dynamic length scale (blue solid line): $\lambda^*\sim 0.07\xi_D+0.02$; linear fit to the square root of the decoupling factor (red dashed line): $\lambda^*\sim 0.07(D\tau^*)^{1/2}$. Inset: log-log plot of the decay length as a function of time for volume fractions (from left) ϕ=0.5, 0.53, 0.55, and 0.56 with power-law fits $\lambda^*\sim t^\gamma$, γ=0.6 (ϕ=0.5), 0.58 (ϕ=0.53), 0.50 (ϕ=0.55), and 0.46 (ϕ=0.56).

Only a few experimental results for hard sphere colloids at high volume fractions [3–6] and dense depletion gels [33,34] have been reported. The emphasis has been on the van Hove functions at an intermediate time scale corresponding to the peak of the non-Gaussian parameter. This falls in the late-β–early-α process crossover regime where particles have moved only a small fraction of their diameter. We are not aware of any data at the α relaxation time. Over the $G_s(r,t)>10^{-5}$ range typically measured, exponential tails emerge with characteristic decay lengths that are a *fraction* of a particle diameter. The decay lengths do grow with time and volume fraction. An exponential (Poisson) distribution of jumping times was deduced for dense depletion gels [33,34], which is consistent with the NLE theory.

B. Jump length scale

We define an α *relaxation time jump length*, λ^*, as the characteristic displacement of the fast trajectories that compose the tail corresponding to $G_s(r,t=\tau^*)\propto e^{-r/\lambda^*}$. Results are shown in Fig. 4. The jump length increases nonlinearly with volume fraction, from a roughly constant value of ~0.05 for

$\phi < 0.48$ ($F_B \leq k_B T$) to roughly one-fourth of a particle diameter at the highest volume fraction, $\phi = 0.57$. Since the exponential tail characterizes the fast hopping subpopulation, one might expect the growth of λ^* with ϕ to be strongly correlated with measures of the non-Gaussian behavior. Previously, we calculated [8] a length scale for recovery of Fickian diffusion, ξ_D, from fitting our numerical results for the wave-vector dependence of the decay time of the incoherent dynamic structure factor to the expression $\tau^{-1}(k) \approx Dk^2[1+k^2(\xi_D/2\pi)^2]^{-1}$. This form interpolates between diffusive behavior at small wave vectors and a length-scale independent relaxation time at high wave vectors. Figure 4 shows that the α relaxation jump length λ^* is proportional to the diffusive recovery length scale ξ_D, as well as to the length scale for decoupling of relaxation and self-diffusion, $\sqrt{D\tau^*}$. Hence, the fast hopping particles that produce the exponential tail in $G_s(r,t)$ are also responsible for the non-Gaussian behavior in the incoherent dynamic structure factor, and multiple measures of non-Gaussian behavior have the same physical origin in our theory. At the empirical MCT temperature, binary Lennard-Jones mixture (BLJM) simulations find the decay length at the mean α time is roughly 0.25σ [14]. This is in remarkably good accord with the results in Fig. 4 since the empirical MCT volume fraction in the theory [8,34] is $\phi \sim 0.57-0.58$.

A time dependence of the exponential decay parameter is found in simulations and experiments [14,32]. Theoretical results for $\lambda(t)$ for various volume fractions are shown in the inset of Fig. 4. At intermediate and long [but before the long-time Fickian crossover in $G_s(r,t)$] times, we empirically find an effective power-law growth, $\lambda \sim t^{\gamma}$. The apparent exponent γ decreases from ~ 0.6 to ~ 0.45 with increasing volume fraction. Within the context of our theory, this time dependence is a consequence of the crossover to Fickian diffusion as more mobile particles pass the reaction point and increase the amplitude and range of the van Hove distribution tail. The results can be well represented (not shown [8]) as a linear relationship between the jump length and the particle mean square displacement.

To further investigate the nature of the exponential decay length scale at different times, Fig. 5 presents $\lambda(\phi)$ corresponding to several characteristic displacements of physical interest. The time scale of the non-Gaussian parameter (NGP) peak corresponds closely to a mean square displacement of $r = R^*$ where the cage restoring force of $F_{\text{eff}}(r)$ is maximum [1,8]. At this time and displacement scale, $\lambda \sim 0.03-0.04$ for all volume fractions studied. Confocal microscopy measurements on hard sphere suspensions at $\phi = 0.56$ have been performed at the time scale of the peak of the NGP [5,6]. Exponential tails of the van Hove function were observed, and the characteristic decay length is very close to our theoretical result. In contrast, at the α relaxation time the theoretical decay length grows strongly with volume fraction, such that $\tau^* \propto \exp(33\lambda(\phi))$, i.e., a logarithmic growth of the jump length with the α time. In the logarithmic representation, the bimodality of $P(r,t)$ is qualitatively most pronounced, with equally populated slow and fast peaks, at times near the α relaxation time (inset of Fig. 2). At the α time, the fraction of "fast trajectories" is $\sim 60\%$ for all volume fractions [8].

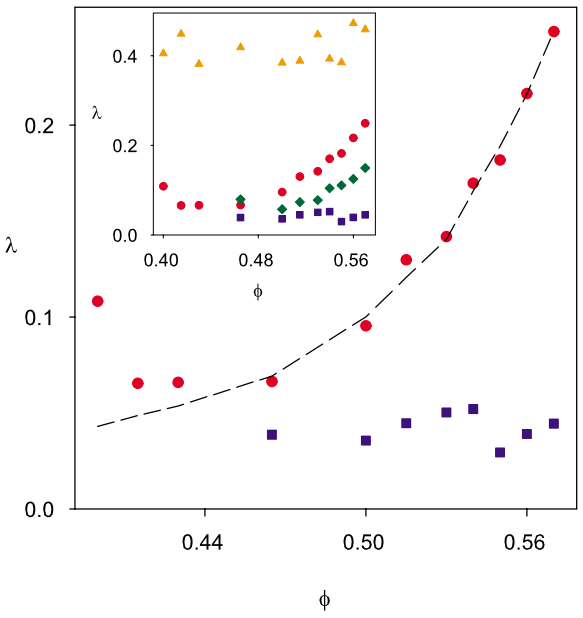

FIG. 5. (Color online) Exponential decay length as a function of volume fraction at times corresponding to $\langle r^2 \rangle^{1/2} = R^*$ (squares) and $t = \tau^*$ (circles), with fit to $\lambda(t=\tau^*) = 0.03 \ln(\tau^*) + 0.1$. Inset: decay length as a function of volume fraction at times corresponding to $\langle r^2 \rangle^{1/2} = R^*$ (squares), $\langle r^2 \rangle^{1/2} = r_B$ (diamonds), $t = \tau^*$ (circles), and $\langle r^2 \rangle^{1/2} = 2$ (triangles).

The inset of Fig. 5 also shows $\lambda(\phi)$ at times corresponding to two other characteristic root-mean-square displacements: the barrier location r_B, which is significantly smaller than the reaction length, and twice the particle diameter. The decay length at r_B is $\sim 0.05-0.15$, growing with volume fraction. In contrast, at $r=2$ the decay length is essentially constant. This indicates that for small ($r = R^*$) and large ($r = 2$) root-mean-square displacements, where the system is predominantly either caged or Fickian, the exponential decay length scale is constant and the shape of the van Hove function does not depend on volume fraction. For intermediate displacements ($r = r_B$, and at $t = \tau^*$), where hopping dynamics and mobility bifurcation are pronounced, the jump length scale is strongly dependent on volume fraction, particularly when there are substantial barriers.

It has recently been suggested [32] based on analysis of a facilitated CTRW model that the time dependence of the exponential decay length of the van Hove function is likely without deep physical meaning. In our theory, the magnitude of λ does depend weakly on the range of $G_s(r,t)$ from which it is extracted. However, within the range over which the exponential fit is good, the deviations do not obscure the qualitative results. In particular, the substantial growth of λ with volume fraction near the α relaxation time, and the near-constant nature of $\lambda(\phi)$ at long times, are clear physical trends. Reference [32] also argues that the time dependence of λ is due to the broad nature of the crossover to Fickian diffusion, a conclusion that does seem to be consistent with our results. In the short-time limit we find, and in the long-time limit we expect, the distribution is best described by a single Gaussian, and at intermediate times the small- and large-r limits of $G_s(r,t)$ are Gaussian-like. The crossover re-

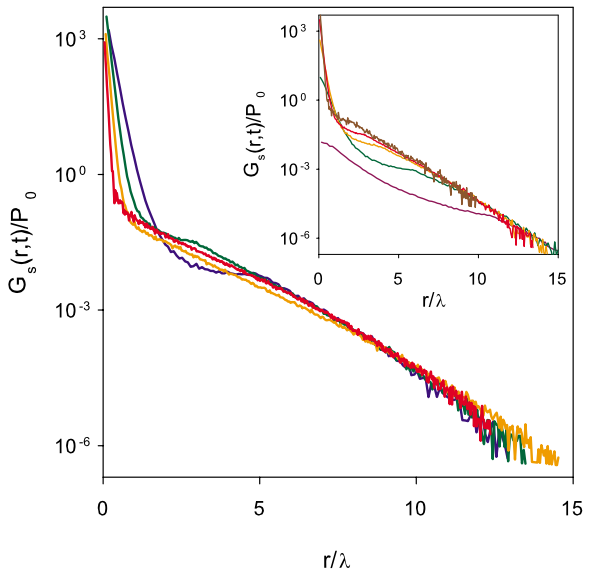

FIG. 6. (Color online) Collapsed van Hove function, normalized on the y axis by a floating parameter and on the x axis by the decay length λ, for ϕ=0.55 at times corresponding to (from right) $\langle r^2\rangle^{1/2}=r_B$, $t=\tau^*$, Kramers time $t=\tau_K$, and $\langle r^2\rangle^{1/2}=2$. Inset: collapsed van Hove function at the α relaxation time for (from bottom) ϕ=0.43, 0.5, 0.53, 0.55, and 0.57.

gion involves substantial populations of slow and fast particles, and the latter is manifest in the exponential tail feature of $G_s(r,t)$.

C. Superposition

Experimental studies of dense depletion gels find a collapse of the time and volume fraction dependences of the van Hove function when normalized by the parameters of the exponential tail [33]. This motivates us to attempt to collapse our theoretical results using the exponential decay length as a scaling variable. The main panel of Fig. 6 shows the results for a high volume fraction of ϕ=0.55 at times corresponding to root-mean-square displacements ranging from the barrier location to 2σ. Vertical shifts were applied to optimize the collapse. For this high entropic barrier system, the exponential decay feature collapses well at the intermediate and long times probed. Deviations occur at large displacements due to the crossover to Fickian diffusion, and at small displacements due to the dominance of the localized or immobile population.

The inset of Fig. 6 attempts to collapse the van Hove function at the α time, $G_s(r,\tau^*)$, over a range of volume fractions for which the barrier varies from 0 to $6.7k_BT$. A quite good collapse occurs for the volume fractions at which activated dynamics is well developed, i.e., when the barrier is $\sim 2k_BT$ or larger ($\phi \geq 0.515$). The lack of collapse for the lower volume fractions is not unexpected since these are in the normal fluid or dynamical crossover regime.

IV. ANALYTIC JUMP MODELS AND LENGTH SCALES

Jump models have a long history in liquid state dynamics [28–30,41]. There are multiple versions that may contain different physics. It is of interest to contrast our numerical NLE theory results with two specific analytic jump models.

A. Torrey model

Motivated by the problem of NMR spin relaxation in liquids, over 50 years ago Torrey developed a simple jump model that appears to have escaped the attention of recent discussions of exponential tails of the van Hove function [30]. Torrey assumed that atoms exist in two states: (a) bound in a deep potential well (trap) with vibrational motion neglected, or (b) in a thermally excited state where the particle undergoes Fickian diffusion with a constant D. Motion consists of a sequence of random trapping and diffusion events described by Poisson statistics with a single mean time between events, τ. The van Hove function involves a sum over all possible numbers of events, n, during a time interval t weighted by the appropriate probabilities,

$$G_s(r,t) = \sum_{n=0}^{\infty} P_n(r) \frac{1}{n!} \left(\frac{t}{\tau}\right)^n e^{-t/\tau}, \tag{5}$$

$$P_n(r) = \int \frac{d\vec{k}}{(2\pi)^3} e^{i\vec{k}\cdot\vec{r}} \left(\frac{1}{1+k^2 D\tau}\right)^n. \tag{6}$$

A single jump process has a simple exponential form

$$P_1(r,t) = \int_0^{\infty} \frac{dt}{\tau} e^{-t/\tau} \frac{e^{-r^2/4Dt}}{(4\pi Dt)^{3/2}} = \frac{e^{-r/\xi}}{4\pi\xi^2 r}, \tag{7}$$

with a characteristic length scale

$$\xi = \sqrt{D\tau}. \tag{8}$$

This jump length is time-independent and proportional to a quantity that describes decoupling of diffusion and "relaxation." It is not determined by either the Torrey or CTRW models, in contrast to our theory [8].

Since the idealization of a discrete jump does not enter our approach, the proper connection with the Torrey model is likely at the level of Eqs. (5) and (6), which correspond to

$$F_s(k,t) = e^{-k^2 Dt/(1+k^2\xi^2)} \equiv e^{-t/\tau(k)}. \tag{9}$$

Indeed, we have shown previously that the form of Eq. (9) does accurately reproduce the full NLE predictions for the incoherent dynamic structure factor [8]. It follows that the basic physical picture underlying our approach is similar to the Torrey trapping and retrapping scenario. In analogy with the physical meaning of Enskog or independent binary collision theory [40,41], our approach should not be thought of as describing just one hopping event, but rather sequences of spatially uncorrelated cage escape events. The latter *do* have a nontrivial spatial character since non-Gaussian dynamics and a characteristic Fickian crossover length are predicted [8].

Equations (5) and (6) can be simplified further by rewriting them as

$$G_s(r,t) = \delta(\vec{r})e^{-\tilde{t}} + \frac{e^{-\tilde{t}}}{2\pi^2}\int_0^\infty dK\, K \sin(k\tilde{r})\left[\exp\left(\frac{\tilde{t}}{1+K^2}\right) - 1\right], \tag{10}$$

where $\tilde{t} \equiv t/\tau$, $\tilde{r} \equiv r/\xi$, and $K \equiv k\xi$. If $\tilde{t} \leq 1$ and $\tilde{r} \leq 1$, corresponding to the intermediate time non-Fickian regime where the exponential tail feature is prominent and ϕ-dependent, the exponential factor in the integrand can be expanded and the series is convergent, thereby yielding

$$G_s(r,t) \simeq \delta(\vec{r})e^{-\tilde{t}} + \frac{\tilde{t}e^{-\tilde{t}}}{4\pi\tilde{\xi}^3}\frac{e^{-\tilde{r}}}{\tilde{r}}. \tag{11}$$

An exponential tail is predicted with amplitude that grows with time, and then eventually vanishes as the dynamics crosses over to Gaussian.

B. General Mori-Zwanzig analysis

We have recently employed Mori-Zwanzig projection operator methods to derive a general expression for the incoherent dynamic structure factor in the long-time Markovian limit where $F_s(k,t) \to e^{-t/\tau(k)}$. The goal was to predict the length scale for the onset of Fickian diffusion. The formally exact expression for the wave-vector-dependent relaxation time is [36]

$$\tau(k) = k^{-2}\beta^2 \int_0^\infty dt \left\langle \sum_j e^{ik[z_j - z_j(t)]} f_j^z f_j^z(t) \right\rangle, \tag{12}$$

where $z_j(t)$ is the z component of the displacement of particle j at time t, and $f_j^z(t)$ is the corresponding force. We adopted a "small" wave-vector expansion thereby yielding

$$\frac{1}{\tau(k)} = \frac{k^2 D}{1 + (k\xi_D)^2}, \tag{13}$$

where ξ_D is a "diffusive" or "viscoelastic" correlation length beyond which Fickian diffusion occurs, and D is the self-diffusion constant. Equation (13) is identical in form to Eq. (9) with

$$\xi_D^2 = \rho^{-1}\beta D \eta_L^s \cong 3\rho^{-1}\beta D \eta_s^s, \tag{14}$$

where η_L^s is the single molecule longitudinal viscosity, which is proportional to τ^*. In principle, the latter is not the same as the true (collective) viscosity, but one expects they are very similar if activated dynamics is dominant [36]. Hence, Eq. (14) corresponds to $\xi_D \propto \sqrt{D\tau^*}$, which is consistent with the numerical NLE theory results and qualitatively the same as the Torrey model.

V. DECOUPLING AND COMPARISON WITH CTRW MODELS AND SIMULATION

A. Continuous-time random walk and kinetically constrained models

The CTRW [31] and KCM [14,23,24,38] types of stochastic models are based on physically motivated, but empirically postulated, dynamical rules. A discrete picture of instantaneous local transport events separated by periods of localization is employed. The simplest way to build in the dynamic facilitation concept of space-dependent mobility is to assume that the first jump occurs more slowly than subsequent jumps. Hence, two distinct mean hopping times, $\langle \tau_p \rangle$ and $\langle \tau_x \rangle$, with $\langle \tau_x \rangle < \langle \tau_p \rangle$, are introduced. The former is the slower "persistence time" for localization prior to the first hopping event, and the latter is the more rapid "exchange" time between events, which vary differently with temperature or density [23,24]. Recent analyses of simulations have defined these time scales in terms of single-particle trajectories [15]. A localization length, r_L, is introduced in the models to account for harmonic vibrations in the trapped state, and jump lengths are characterized by a Gaussian distribution with a width parameter r_J. The idea is that the first hop mimics structural relaxation and controls properties such as viscosity, but self-diffusion requires multiple jumps and is largely determined by the faster subsequent hopping events. This physical picture has been proposed as the origin of decoupling in glassy liquids [14,24]. In its minimalist version, the model has four adjustable parameters, which are not *a priori* related to molecular structure or forces.

In our notation, the above CTRW facilitation model [14] corresponds mathematically to

$$F_s(k,t) = e^{-k^2 r_L^2/6} e^{-t/\langle \tau_p \rangle} + \frac{f(k)}{\alpha f(k) - 1}\left[e^{-t/\langle \tau_p \rangle} - e^{-[1-f(k)]t/\langle \tau_x \rangle}\right], \tag{15}$$

$$f(k) \equiv e^{-k^2 r_L^2/6} e^{-k^2 r_J^2/6}, \quad \alpha \equiv \langle \tau_p \rangle / \langle \tau_x \rangle. \tag{16}$$

In real space, the leading term in Eq. (15) represents "immobile" particles waiting for the first jump, while the second term describes particles that have hopped one or more times and is analytically well represented as an exponential tail with decay length λ in the van Hove function (with logarithmic correction) for intermediate times and distances [14]. To use this model to interpret atomistic simulations, a "jump" or "event" must be (arbitrarily) defined as a particle displacement of some assumed value. Applications to the BLJM models [14,15] employ (small) displacements of order *one-half* a particle diameter or *less*. In applications to colloid gel experiments [32], a jump event is assumed to correspond to an *extremely* small distance, less than *one-tenth* a particle diameter. The latter is the spatial range of the polymer mediated depletion attraction, and is similar to the length scale associated with the maximum cage restoring force of the nonequilibrium free energy of our NLE theory for hard spheres. Defined in this manner, the deduced persistence and exchange times decouple at low temperatures in the BLJM model [14,15], and at high degrees of depletion attraction or volume fraction in colloidal gel-like suspensions [32]. Decoupling is quantified by the parameter α in Eq. (16), which is unity in the normal fluid regime, and grows monotonically with cooling or concentration in the glassy regime [14,15]. For the standard BLJM model, $\alpha \simeq 4$ at the empirical MCT temperature [14]. As the dynamics becomes highly intermittent, the persistence time grows faster and is more broadly distributed than the exchange time [15,24].

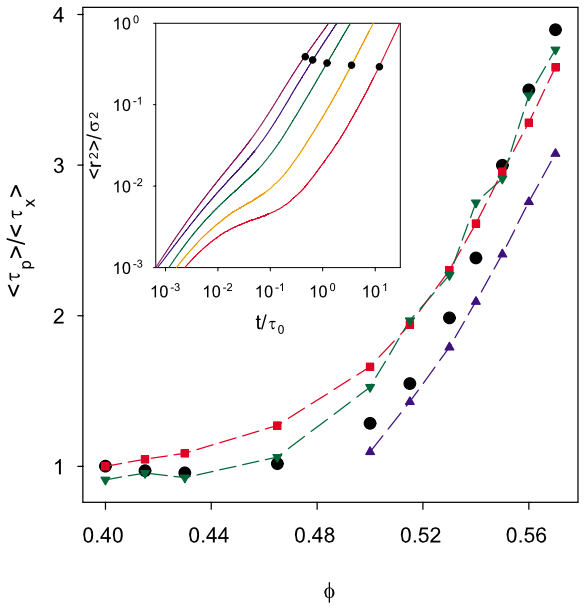

FIG. 7. (Color online) Ratio of the persistence and exchange time (circles) as defined in the text, normalized by the value at $\phi=0.40$, plotted as a function of volume fraction. Dashed lines are normalized $(D\tau^*)^{1/2}$ (squares), ξ_D (up triangles), and $16\lambda^*$ (down triangles). Inset: mean square displacement for (from left) $\phi=0.43$, 0.465, 0.5, 0.53, and 0.55; circles mark the reaction point.

It is not possible to unambiguously compare our theory with discrete jump models since in our approach particles undergo continuous displacements on an effective free-energy landscape that has multiple dynamically relevant energy and length scales. However, we have identified a plausible approach for semiquantitative comparison that is motivated by the recent KCM analysis of an atomistic simulation in Ref. [15]. These workers defined the persistence time as the average time associated with a particle's *first* displacement of a distance equal to its *radius*. The exchange time is the average time to displace an *additional* particle radius. We analyze our results based on this perspective.

B. Decoupling in the NLE theory and comparison with CTRW models

In the NLE theory, the mean reaction time, $\langle\tau_{rxn}\rangle$, is the average time for trajectories to surmount the barrier and first attain the reaction displacement $r^{\dagger}\sim 0.5-0.6$. We have shown this time is nearly identical [8] to the structural relaxation time defined by $F_s(k^*,t=\tau^*)=e^{-1}$. Thus $\langle\tau_{rxn}\rangle$ is the analog of a persistence time, and we identify $\langle\tau_p\rangle\equiv\langle\tau_{rxn}\rangle$. We have also studied a mean diffusion time, $\langle\tau_{\rm diff}\rangle$, for particles to displace to $r=1$, comprising both the dynamics on the effective free energy landscape and a period of renormalized three-dimensional Fickian diffusion [8]. We adopt as a simple estimate of an exchange time $\langle\tau_x\rangle\equiv\langle\tau_{\rm diff}\rangle-\langle\tau_{rxn}\rangle$.

Figure 7 shows our calculations of the ratio $\alpha\equiv\langle\tau_p\rangle/\langle\tau_x\rangle$ reduced by its value at the lowest volume fraction studied, $\phi=0.4$ (no barrier, normal fluid regime). In the absence of an entropic barrier, this measure of decoupling shows no volume fraction dependence. However, the ratio grows as the barrier exceeds $\sim kT$, and at $\phi=0.57$ reaches $\alpha\sim 4$. We note that $\phi\sim 0.57-0.58$ is the empirically determined ideal MCT transition of our theory [8,34]. Hence, the predicted magnitude of decoupling is in remarkable agreement with its analog extracted from a recent simulation of the classic BLJM at the empirical $T_{\rm MCT}$ [14]. Moreover, the shape of the decoupling curve in Fig. 7 is quite similar to that found for several BLJM simulations [14–17,21] if one makes the natural correspondence $T_{\rm MCT}/T\leftrightarrow\phi/\phi_{\rm MCT}$. Figure 7 also demonstrates that $\langle\tau_p\rangle/\langle\tau_x\rangle$ is numerically very similar to our prior results [8] for the diffusive dynamic length scale, ξ_D, as extracted from the wave-vector dependence of the incoherent dynamic structure factor relaxation time, and also the decoupling factor, $\sqrt{D\tau^*}$. Moreover, we find $\langle\tau_p\rangle/\langle\tau_x\rangle$ is roughly proportional to the α time exponential decay length, λ^*.

To interpret the significance of these results, we summarize the physics underlying decoupling in our theory [1,8]. There are three key points.

(i) Decoupling does not arise from the naive idea that diffusion and relaxation are simply different temporal moments of a Poisson hopping time distribution. Rather, it is largely our "dynamic constraint release" idea that particle trajectories of highly varying mobilities become diffusive, governed by a common mean hopping friction constant, beyond a common reaction displacement associated with a distributed (reaction) time scale. The hopping friction follows from averaging over all trajectories before the reaction point. Hence, one might view the analog of the mean exchange time as a subtle reaveraging of trajectories in a manner distinct from determination of the persistence ($\sim\tau^*$) time. The concept of highly local, irreversible activated hopping motions on the subparticle diameter length scale as the basic mechanism of the α relaxation process has recently acquired direct experimental support based on confocal microscopy observations for very high volume fraction colloid glasses [43].

(ii) The decoupling of our $\langle\tau_p\rangle$ and $\langle\tau_x\rangle$ is related to the different volume fraction dependences of the reaction and diffusion times, i.e., differences in mobility on different length scales. Distributions of the reaction and diffusion times are shown in Fig. 8. At the smallest volume fraction, the two distributions have very similar, log-normal shapes. With increasing volume fraction, the reaction time distribution develops a fast hopping tail and transforms to a nearly Poisson form. In contrast, the diffusion time distribution retains its log-normal shape. Although both mean times become substantially longer, the increase in the reaction time is greater.

(iii) The particle mean square displacements are shown in the inset of Fig. 7. Transport on the reaction and smaller length scales is not Fickian, and the "hopping" rate (local slope of MSD) is predicted to be a continuous and nonmonotonic function of particle displacement [1,8], the details of which are in good agreement with colloidal experiments [37]. Hence, a slower "first jump" is a natural consequence of the need to surmount a barrier located at $r_B\sim 0.3-0.4$. The second "jump," following the crossover to a linear Langevin description, occurs on a flat effective free energy surface with a renormalized (smaller) diffusion constant. Thus, it is not surprising that $\langle\tau_p\rangle$ has a stronger volume fraction dependence than $\langle\tau_x\rangle$.

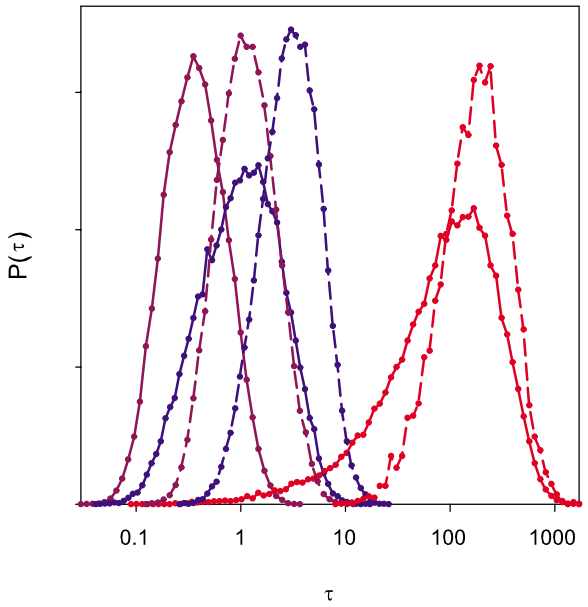

FIG. 8. (Color online) Probability distributions for the reaction time (solid lines) and diffusion time (dashed lines), ϕ=0.43, 0.5, and 0.57 (from left).

We cannot definitely state how our physical picture connects to dynamic facilitation concepts and KCMs. However, a key common idea is that mobility is a function of particle displacement [8,23,36,38,44]. A practical limitation to drawing more precise conclusions is that the KCMs are a coarse grained, discrete jump description of a continuum fluid, which is only just beginning to be applied on the subparticle size length scale. In our opinion, liquid structure and molecular details cannot be irrelevant on such length scales.

VI. CONCLUSION

We have analyzed the numerical predictions of the stochastic nonlinear Langevin theory of activated dynamics for the real-space van Hove function in hard sphere fluids and suspensions. Detailed summaries of our results, and comparison with other theories, simulations, and experiments, have been given in prior sections. Overall, we believe the theory provides a good account of the exponential tail feature of the van Hove function, in terms of both the absolute magnitude of the decay length and its dependence on volume fraction. The primary origin of inaccuracies in the theory is likely the adoption of an abrupt crossover from motion on a *dynamical* free energy landscape to three-dimensional Fickian diffusion. Space-time correlated activated hopping dynamics on length scales well beyond the particle size, and the possible distributed nature of local caging constraints [e.g., spatial environment fluctuations of $F_{\rm eff}(r)$], are not presently included in the NLE theory. Whether such effects are essential for understanding the existing colloidal experiments and computer simulations that probe only a glassy dynamical precursor regime is not at all obvious to us. In our opinion, there is no compelling evidence that the answer is in the affirmative for single-particle dynamics.

We suggest that the recent analyses of simulations and confocal experiments based on facilitated and discrete CTRW models should be more thoroughly explored in order to establish the robustness of the deduced conclusions to varying the arbitrary definition of a particle "jump." This suggestion is also applicable to the analysis of our continuous-space NLE theory in the discrete framework of "exchange" and "persistence" events. We also suggest that many new confocal microscopy experiments (simulations) be performed on model hard sphere colloidal suspensions (fluids) to systematically test our prior [1,8] and present predictions as a function of time, displacement, and volume fraction. The issue of how to define an event or jump seems even more problematic for depletion particle gels in which slow dynamics is controlled by very short-range attractions. The application of our NLE theory to explore the non-Gaussian fluctuation dynamics and real-space van Hove function of such systems is of great interest, especially given the emerging experimental capability to probe single-particle dynamics using confocal microscopy. Efforts are underway in this direction.

ACKNOWLEDGMENTS

We gratefully acknowledge funding from the Department of Energy–Basic Energy Sciences via Grant No. DE-FG02-07ER46471 obtained through the Frederick Seitz Materials Research Laboratory. We thank David Chandler for helpful correspondence concerning Ref. [15].

[1] K. S. Schweizer, Curr. Opin. Colloid Interface Sci. **12**, 297 (2007).
[2] W. van Megen, T. C. Mortensen, S. R. Williams, and J. Muller, Phys. Rev. E **58**, 6073 (1998); W. van Megen, T. C. Mortensen, and G. Bryant, *ibid.* **72**, 031402 (2005).
[3] A. Kaspar, E. Bartsch, and H. Sillescu, Langmuir **14**, 5004 (1998).
[4] W. Kegel and A. van Blaaderen, Science **287**, 290 (2000).
[5] E. R. Weeks, J. C. Crocker, A. C. Levitt, A. Schofield, and D. A. Weitz, Science **287**, 627 (2000).
[6] E. R. Weeks and D. A. Weitz, Chem. Phys. **284**, 361 (2002); Phys. Rev. Lett. **89**, 095704 (2002).
[7] L. J. Kauffman and D. A. Weitz, J. Chem. Phys. **125**, 074716 (2006).
[8] E. J. Saltzman and K. S. Schweizer, J. Chem. Phys. **125**, 044509 (2006); Phys. Rev. E **74**, 061501 (2006).
[9] S. K. Kumar, G. Szamel, and J. F. Douglas, J. Chem. Phys. **124**, 214501 (2006).
[10] D. R. Reichman, E. Rabani, and P. L. Geissler, J. Phys. Chem. B **109**, 14 654 (2005).
[11] W. K. Krekelberg, J. Mittal, V. Ganesan, and T. M. Truskett, J. Chem. Phys. **127**, 044502 (2007).

[12] W. Kob, C. Donati, S. J. Plimpton, P. H. Poole, and S. C. Glotzer, Phys. Rev. Lett. **79**, 2827 (1997); T. Odagaki and Y. Hiwatari, Phys. Rev. A **41**, 929 (1990).
[13] D. A. Stariolo and G. Fabricius, J. Chem. Phys. **125**, 064505 (2006).
[14] P. Chaudhuri, L. Berthier, and W. Kob, Phys. Rev. Lett. **99**, 060604 (2007).
[15] L. O. Hedges, L. Maibaum, D. Chandler, and J. P. Garrahan, J. Chem. Phys. **127**, 211101 (2007).
[16] R. Yamamoto and A. Onuki, Phys. Rev. Lett. **81**, 4915 (1998).
[17] E. Flenner and G. Szamel, Phys. Rev. E **72**, 031508 (2005).
[18] G. Szamel and E. Flenner, Europhys. Lett. **67**, 779 (2004).
[19] L. Berthier and W. Kob, J. Phys.: Condens. Matter **19**, 205130 (2007).
[20] L. Berthier, Phys. Rev. E **69**, 020201(R) (2004).
[21] E. Flenner and G. Szamel, Phys. Rev. E **72**, 011205 (2005).
[22] G. Szamel and E. Flenner, Phys. Rev. E **73**, 011504 (2006).
[23] Y. Jung, J. P. Garrahan, and D. Chandler, Phys. Rev. E **69**, 061205 (2004); J. Chem. Phys. **123**, 084509 (2005).
[24] L. Berthier, D. Chandler, and J. P. Garrahan, Europhys. Lett. **69**, 320 (2005).
[25] W. Götze and L. Sjögren, Rep. Prog. Phys. **55**, 242 (1992).
[26] S. Das, Rev. Mod. Phys. **76**, 785 (2005).
[27] L. van Hove, Phys. Rev. **95**, 249 (1954).
[28] C. T. Chudley and R. J. Elliott, Proc. Phys. Soc. London **77**, 353 (1961).
[29] K. S. Singwi and A. Sjolander, Phys. Rev. **120**, 1093 (1960).
[30] H. C. Torrey, Phys. Rev. **92**, 962 (1953).
[31] E. W. Monroll and G. H. Weiss, J. Math. Phys. **6**, 167 (1965).
[32] P. Chaudhuri, Y. Gau, L. Berthier, M. Kilfoil, and W. Kob, e-print arXiv:0712.0887v2, J. Phys.: Condens. Matter (to be published).
[33] Y. Gao and M. L. Kilfoil, Phys. Rev. Lett. **99**, 078301 (2007).
[34] K. S. Schweizer and E. J. Saltzman, J. Chem. Phys. **119**, 1181 (2003); E. J. Saltzman and K. S. Schweizer, *ibid.* **119**, 1197 (2003).
[35] K. S. Schweizer, J. Chem. Phys. **123**, 244501 (2005).
[36] K. S. Schweizer and E. J. Saltzman, J. Phys. Chem. B **108**, 19729 (2004).
[37] E. J. Saltzman, G. Yatsenko, and K. S. Schweizer, J. Phys.: Condens. Matter (to be published).
[38] F. Ritort and P. Solich, Adv. Phys. **52**, 219 (2003).
[39] A. J. Archer and M. Rauscher, J. Phys. A **37**, 9325 (2004); U. M. B. Marconi and P. Tarazona, J. Chem. Phys. **110**, 8032 (1999).
[40] E. G. D. Cohen, R. Verberg, and I. M. de Schepper, Physica A **251**, 251 (1998).
[41] J. P. Hansen and I. R. McDonald, *Theory of Simple Liquids* (Academic, London, 1986).
[42] T. R. Kirkpatrick and P. G. Wolynes, Phys. Rev. A **35**, 3072 (1987).
[43] P. Schall, D. A. Weitz, and F. Spaepen, Science **318**, 1895 (2007).
[44] S. Whitelam and J. P. Garrahan, J. Phys. Chem. B **108**, 6611 (2004)